

DESIGN CALCULATIONS OF HELIOSTAT FIELD LAYOUT FOR SOLAR THERMAL POWER GENERATION

¹HNIN WAH, ²NANG SAW YUZANA KYAING

^{1,2}Electrical Power Engineering Department, Mandalay Technological University, Myanmar
E-mail: ¹hninwahr88@gmail.com, ²nansawyuzana@gmail.com

Abstract- The aim of this paper is to design the heliostat field layout of solar thermal generation for a CSP plant, based on the central power tower technology. In this design, the radial staggered pattern is proposed to reduce the shadowing and blocking losses. Its solar field consists of 1150 heliostats around a 95m tall tower and each heliostat has a 121m² reflecting area. The power plant is designed to produce an output of 56MW_{th} thermal power with molten salt storage system. The coordinates of the chose location for this plant are 19.7633° (Latitude) and 96.0785° (Longitude), which is a city called Naypyitaw, Myanmar. To evaluate the available solar thermal power received at the central receiver, the optical efficiency which is the product of the mirror reflectivity, the atmospheric attenuation efficiency, the shadowing and blocking efficiency and the cosine efficiency is proposed as well. Results show that the annual optical efficiency increases and the minimum value of thermal power received on the tower receiver is greater than required power.

Keywords- 56 MW_{th}, Atmospheric attenuation efficiency, Central power tower technology, Cosine efficiency, Heliostat field layout, Molten salt storage system, Optical efficiency, Shadowing and blocking, Solar thermal power.

I. INTRODUCTION

Concentrated solar power (CSP) technologies are expected to lead the power production in the future in many countries. Among CSP technologies, central receiver system (CRS) or central power tower is an attractive method to achieve tremendously huge power and high concentration of solar irradiance for electricity generation or thermal processes. This system involves the use of many individual sun-tracking mirrors or heliostats to reflect and to superpose the concentrated sunlight at a common receiver attached on top of the central tower. The performance of the heliostat field is defined in terms of the optical efficiency which is the ratio of the net power absorbed by the receiver to the power incident normally on the field. The optical losses from the heliostat field take into account the losses, such as cosine, shadowing and blocking, due to the field layout. Most of the heliostat field is designed in radial stagger pattern. This arrangement ensures that no heliostat is consigned in front of another heliostat in adjacent rings because reflected beam from the heliostats can pass directly to the receiver between adjacent neighbors [1]. Since the heliostat field provides the reflected energy, 50% of the total cost of the power plant and 40% of the energy losses are associated with the heliostat field, the design of heliostat field layout is crucially important [2,3]. Therefore, the annual optical efficiency that evaluates the performance of the heliostat field needs to be calculated accurately.

Several studies have revealed that the radial stagger arrangement is the most efficient for a given land area as it cuts down the land usage and atmospheric attenuation losses. Hence, it contributes to the most expedient distribution for heliostat fields. Lipps et al. [4] presented staggered and cornfield configurations, but the conclusion of this work shows that the radial

staggered configuration generates more efficient layouts due to the lower losses related to shadowing and blocking. Collado et al. [5] presented a simplified version of this algorithm that considered the spacing between the rings of a zone constant. In order to reduce the shadowing and blocking losses, and to keep the minimum distance for mechanical constraints, the algorithm proposed a parameter 'desp' to define the minimum distance between the heliostats. For this algorithm, the first step is the calculation of the parameters that define each of the zones in the field (azimuth spacing, the radius of the first row in the zone, number of heliostats per row and the number of rows in the zone). Currently, radial staggered type layout is used to design real heliostat field.

This paper is organized as follows. Heliostat field layout design is described in Section 2. In Section 3, the computation of the optical efficiency is introduced. The modeling of the incident on the tower receiver is proposed in Section 4. In Section 5, the simulation results are shown. Finally, conclusions are drawn in Section 6.

II. HELIOSTAT FIELD LAYOUT DESIGN

Most heliostat field layout designs take a radial stagger pattern according to the fact that each heliostat can move freely and the heliostats standing between two heliostats of the front ring reduce the blocking. Most approaches to improve the layout design of the heliostat field are based on the radial stagger concept. In this subsection, the method to deploy a radial staggered heliostat field and to calculate various parameters such as the characteristic diameter, radial spacing, azimuthal spacing, number of rows and number of heliostats is presented. The variables used to define the heliostat are illustrated in Figure 1 [6].

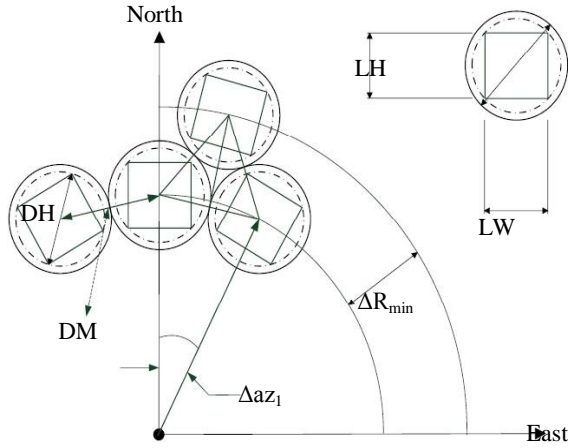


Figure 1. Fundamental definitions in the heliostat field [6]

2.1. The Characteristic Diameter

The characteristic diameter is the distance between the center of the adjacent heliostats, and it can be calculated with the following equation [6]:

$$DM = \sqrt{l_w^2 + l_h^2} + \text{desp} \quad (1)$$

where DM is the characteristic diameter of the heliostat in m, l_w and l_h are the width and height of the heliostat in m, and desp is any additional separation distance between adjacent heliostats.

2.2. The Radial and Azimuth Spacing

The minimum radius of the heliostats should ensure that adjacent heliostats do not happen mechanical collisions, and is given as [6]:

$$\Delta R_{\min} = DM \times \cos 30^\circ \quad (2)$$

Based on the number of heliostats in each row of the first zone, radial distance from the tower to the first row of the heliostats (R_1) can be calculated as follows [6]:

$$R_1 = N_{hel_1} \frac{DM}{2\pi} \quad (3)$$

where N_{hel_1} is the number of heliostats within each row of the first zone.

The azimuth angular spacing for the first zone of the heliostat field can be determined by [6]:

$$\Delta az_1 = 2 \sin^{-1} \frac{DM}{2R_1} \quad (4)$$

where Δaz_1 is the azimuth angular spacing for the first zone in rad.

Due to the radially staggered configuration, the distance between two adjacent mirrors (length in meters) depends on their radial distance from the tower. Consequently, as the rows get further away from the tower, the space between their heliostats increases. Eventually, spaces between the mirrors become greater than DM making it possible to place extra mirrors between two adjoining mirrors in the same row. A zone is considered to be completed as the possibility of the addition of extra mirrors within

its final row. Consequently, the azimuth angular spacing for the i^{th} zone can be determined by [6]:

$$\Delta az_i = \frac{\Delta az_1}{2^{i-1}} \quad (5)$$

where Δaz_i is the azimuth angular spacing for the i^{th} zone in rad.

The radial distance from the tower to the first row of the i^{th} zone is calculated such that [6]:

$$R_i = 2^{i-1} \frac{DM}{\Delta az_1} \quad (6)$$

where R_i is the radius of the first row for the i^{th} zone in m.

Using equations 2 through 6, the radial and azimuth angular spacing for different zones from the tower can be calculated.

2.3. Number of Rows and Heliostats

The number of rows for the i^{th} zone is determined by [6]:

$$N_{row_i} = \frac{R_{i+1} - R_i}{\Delta R_{\min}} \quad (7)$$

where N_{row_i} is the number of rows of heliostats for i^{th} zone of the field.

The number of heliostats for each row within the i^{th} zone is calculated as [6]:

$$N_{hel_i} = \frac{2\pi}{\Delta az_i} \quad (8)$$

where N_{hel_i} is the number of heliostats in each row within the i^{th} zone.

III. MODEL OF THE OPTICAL EFFICIENCY

The optical efficiency, η_{opt} measures the energy loss of the heliostat field. In general, the optical efficiency is calculated by [7]:

$$\eta_{opt} = \eta_{at} \times \eta_{ref} \times \eta_{s\&b} \times \eta_{cos} \quad (9)$$

where η_{at} is atmospheric attenuation efficiency, η_{ref} is mirror reflectivity, $\eta_{s\&b}$ is shadowing and blocking efficiency and η_{cos} is cosine efficiency. Among them, the value of mirror reflectivity depending on the heliostat reflective rate can be set to a constant ($\eta_{ref} = 0.95$ is adopted here), the others are influenced by the heliostat field configuration, the height of the receiver or other factors related. As a result, four types of efficiency except η_{ref} need to be computed to determine the optical efficiency.

3.1. The Atmospheric Attenuation Efficiency, η_{at}

The effect that some of the energy of the reflected rays are scattered and absorbed by the atmosphere is referred as atmospheric attenuation loss. The atmospheric transmission efficiency strongly depends on the weather condition and the distance between the heliostat and the receiver. For a visual distance of

about 40 km, the atmospheric transmission efficiency can be calculated simply as a function of the distance between the heliostat and the receiver in meters as follow [7].

If $d \leq 1000\text{m}$,

$$\eta_{\text{at}} = 0.99321 - 0.0001176d + 1.97 \times 10^{-8} d^2 \quad (10)$$

If $d > 1000\text{m}$,

$$\eta_{\text{at}} = e^{-0.0001106d} \quad (11)$$

where d is the distance between the heliostat and the receiver. The atmospheric attenuation efficiency (η_{at}) can be calculated by using equations (10) and (11).

3.2. The Shadowing and Blocking Efficiency

Shadowing occurs when a shadow is cast by a heliostat onto a neighboring heliostat. Therefore, all the incident solar flux doesn't reach the reflector. Blocking losses occur when a heliostat's reflected flux is blocked by a heliostat in the foreground. The detailed, time dependent calculations of shadowing and blocking require complex procedures involving intricate ray tracing of individual heliostats. This sort of analysis is beyond the scope of this paper. Therefore, typical yearly average value is used. Annual average shadowing and blocking loss is about 5.60% [3].

3.3. The Cosine Efficiency

The most significant loss in the heliostat field is due to the angle between the incident solar beam radiation, and a vector normal to the surface of the heliostat which is called the cosine effect. Therefore, it depends on both sun and heliostat positions.

a. Solar position

The solar position is very important because the sun is changing hourly during a day and daily during the year, so it is necessary to model the solar coordinate systems during the year through solar angles.

The solar declination is calculated by [8]:

$$\delta_s = 23.45 \sin\left(\frac{360}{365}(284 + N)\right) \quad (12)$$

where N is the number of days during the year starting from the 1st of January.

The solar hour angle (h_s) is calculated using the following equation, where the solar hour, also known as solar time, is the apparent solar time of the day [9].

$$h_s = (\text{Solar hour} - 12) \times 15^\circ \quad (13)$$

The solar altitude angle (α_s) is computed with the equation (14), where all the parameters are calculated and defined previously above [10]:

$$\alpha_s = \sin^{-1} [\cosh(h_s) \cdot \cos(\delta_s) \cdot \cos(\phi_{\text{lat}}) + \sin(\delta_s) \cdot \sin(\phi_{\text{lat}})] \quad (14)$$

The solar zenith angle (θ_z) is obtained as a function of α_s [9].

$$\theta_z = 90^\circ - \alpha_s \quad (15)$$

The solar azimuth angle (ϕ_s) is calculated by considering a solar azimuth factor (ϕ') and the solar hour angle conditions [8].

$$\phi' = \sin^{-1} \left(\frac{\cos \delta_s \times \sinh_s}{\sin \theta_z} \right) \quad (16)$$

The solar hour angle conditions are [8]:

$$\text{If } \cosh_s \geq \left(\frac{\tan \delta_s}{\tan \phi_{\text{lat}}} \right), \quad \phi_s = 180^\circ - \phi' \quad (17)$$

$$\text{Else } \cosh_s \leq \left(\frac{\tan \delta_s}{\tan \phi_{\text{lat}}} \right), \quad \phi_s = 180^\circ + \phi' \quad (18)$$

The surface azimuth angle (ϕ_{surf}) can be obtained by [8]:

$$\text{If } \phi_s - \phi' > 0, \quad \phi_{\text{surf}} = \phi' + 90^\circ \quad (19)$$

$$\text{Else } \phi_s - \phi' < 0, \quad \phi_{\text{surf}} = \phi' - 90^\circ \quad (20)$$

Using equations (12) through (20), the solar declination (δ_s), the solar altitude angle (α_s), the solar hour angle (h_s), the solar azimuth angle (ϕ_s) and the solar zenith angle (θ_z) can be calculated to find the cosine efficiency.

b. Heliostat position

The solar altitude angle of the tower receiver for each heliostat (α_{tr}) which is defined by the tower height (H_t), the height of each heliostat (H_h) and the distance of each heliostat from the tower base (R) is calculated and illustrated in Figure 2 [11].

$$\alpha_{\text{tr}} = \tan^{-1} \left(\frac{H_t - H_h}{R} \right) \quad (21)$$

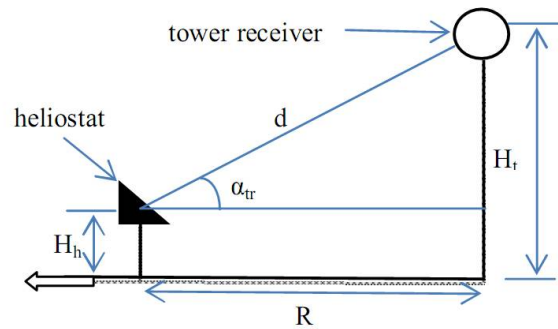


Fig 2. Solar altitude angle of tower receiver [11]

For calculating the distance of each heliostat from the tower receiver (d), the Pythagorean Theorem is used.

$$d = \sqrt{R^2 + (H_t - H_h)^2} \quad (22)$$

In order to reflect the incident radiation on each heliostat and direct it to the tower receiver, the rotation angle of them is calculated by [12]:

$$\beta_{\text{hs}} = \frac{\alpha_{\text{tr}} + \alpha_s}{2} \quad (23)$$

The solar incidence angle on each heliostat (θ_s) is calculated by [12]:

$$\theta_s = \cos^{-1}[(\sin\phi_{lat}.\sin\delta_s.\cos\beta_{hs})-(\cos\phi_{lat}.\sin\delta_s.\sin\beta_{hs}.\cos\varphi_{surf}) + (\cos\phi_{lat}.\cos\delta_s.\cosh_s.\cos\beta_{hs})+(\sin\phi_{lat}.\cos\delta_s.\cosh_s.\sin\beta_{hs}.\cos\varphi_{surf})+(\cos\delta_s.\sinh_s.\sin\beta_{hs}.\sin\varphi_{surf})] \quad (24)$$

c. Tower receiver design

In order to absorb the maximum reflected radiation from the solar field and get the expected thermal energy on the receiver to warm up the molten salts to desired temperatures, the tower receiver design is very important. Therefore, the receiving angle of the reflected rays on the receiver aperture (θ_R) and the angle between reflected sun rays and the vertical direction (λ_s) are important to define and calculate as shown in Figure 3 [13].

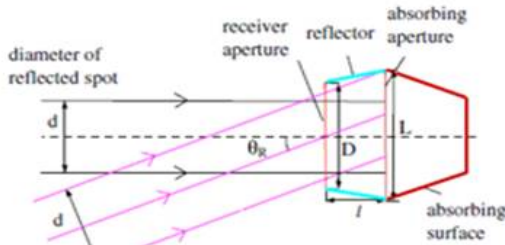


Figure 3. Acceptance angle of the receiver [13]

$$\theta_R = \sin^{-1}\left(\frac{-2dl + L\sqrt{4l^2 + L^2 - d^2}}{4l^2 + L^2}\right) \quad (25)$$

$$\lambda_s = 90^\circ - \theta_R \quad (26)$$

where d is the diameter of reflected spot, l is the reflector length and L is the absorbing aperture height.

After getting all the solar angles needed and defining the solar field layout, the optical efficiency of the heliostat field is calculated by [13]:

$$\eta_{\cos} = \frac{\sqrt{2}}{2} (\sin\alpha_s.\cos\lambda_s - \cos(\varphi_{surf} - \varphi_s).\cos\alpha_s.\sin\lambda_s + 1)^{0.5} \quad (27)$$

Substituting equations (14), (17), (18), (19), (20) and (26) in equation (27), the cosine efficiency can be calculated.

IV. SOLAR RADIATION

For modeling the incident radiation on the tower receiver, it is mandatory to calculate the extraterrestrial radiation (G_o), the beam irradiance normal to the solar beam (B_{oc}) and the solar beam irradiation on an inclined surface (B_{ic}), and to define the Linke atmospheric turbidity factor (Tlk), the relative optical air mass (m_{opt}) and the Rayleigh optical thickness at air mass m_{opt} (d_{rm}). The

extraterrestrial radiation normal to the solar beam (G_o) is computed as a function of the solar constant ($G_{sc} = 1367 \text{ W.m}^{-2}$) [12],

$$G_o = G_{sc}\left(1 + 0.033 \cos \frac{360N}{365}\right) \cos \theta_z \quad (28)$$

The beam irradiance normal to the solar beam (B_{oc}) is calculated through equation (29) [11]:

$$B_{oc} = G_o \cdot \exp(-0.8662 \cdot \text{Tlk} \cdot m_{opt} \cdot d_{rm}) \quad (29)$$

For computing the relative optical air mass (m_{opt}), a condition for the solar altitude angle (α_s) is used:

$$\text{If } \alpha_s > 30^\circ, m_{opt} = \frac{1}{\sin \alpha_s} \quad (30)$$

Else $\alpha_s < 30^\circ,$

$$m_{opt} = \frac{1.002432 \sin^2 \alpha_s + 0.148386 \sin \alpha_s + 0.0096467}{\sin^3 \alpha_s + 0.149864 \sin^2 \alpha_s + 0.0102963 \sin \alpha_s + 0.000303978} \quad (31)$$

The Rayleigh optical thickness at air mass m (d_{rm}) is obtained with two empirical equations [11]:

$$\text{If } m_{opt} \leq 20, \quad d_{rm} = \frac{1}{6.6296 + 1.7513m_{opt} - 0.1202m_{opt}^2 + 0.0065m_{opt}^3 - 0.00013m_{opt}^4} \quad (32)$$

Else $m_{opt} > 20,$

$$d_{rm} = \frac{1}{10.04 + 0.718m_{opt}} \quad (33)$$

The solar beam irradiation on an inclined surface (B_{ic}) is given by:

$$B_{ic} = B_{oc} \sin \theta_s \quad (34)$$

After obtaining the value of irradiation for one year and for each heliostat, the solar thermal power received at the tower receiver (Q_{tr}) is calculated as the sum of this irradiation for each heliostat j and for each hour of the year i multiplied by each heliostat area (A_{hs}) and its optical efficiency (η_{opt}),

$$Q_{tr} = \sum_{i=[1, N]} \sum_{j=[1, N_h]} B_{ic}(i, j) \cdot A_{hs} \cdot \eta_{opt} \quad (35)$$

where N_h is the total number of heliostats.

V. RESULTS

To set up the radial configuration, several initial design parameters are required. All initial assumptions and design variables to set up and analyze the optical efficiency of the field are tabulated in Table 1. The field layout of the radial stagger pattern is shown in Figure 4. Each zone is distinguished with different color. The first row consists of 25 heliostats. As seen, field density

reduces within each zone by moving outward away from the center of the field (tower). The first zone contains 100 heliostats spread equally in 4 rows. The second zone contains 450 heliostats distributed equally within 9 rows. Finally, the third zone contains 600 heliostats distributed equally within 6 rows. In total, this design field layout contains 19 rows and 1150 heliostats around a 95m tall tower, and each heliostat has a 121m² reflecting area. The required land area that was calculated from the center of the tower towards the last row of the heliostat field is 636.6682m². This land area is dependent on the radial and azimuthal spacing. Since radial staggered pattern was used for heliostat field layout, the land area and shadowing and blocking losses are reduced. As shown in Table 1, the result of annual optical efficiency (66.42 %) could reach up to more than that of the PS10 field, which is about 64.06% [13]. As a result, the overall optical efficiency of the field is raised.

Table 1. The Details and Results of Field Layout

Details of the Field	
Latitude	19.7633°
Tower Height	95 m
Heliostat Height	7 m
Heliostat Size	11×1m ²
Number of Heliostat	1150
Separation Distance	0.2 m
Absorbing Aperture Height	20 m
Diameter of Reflected Spot	10 m
Reflector length	8 m
Results	
Attenuation Efficiency	0.9690
Cosine Efficiency	0.8252
Optical Efficiency	0.6642

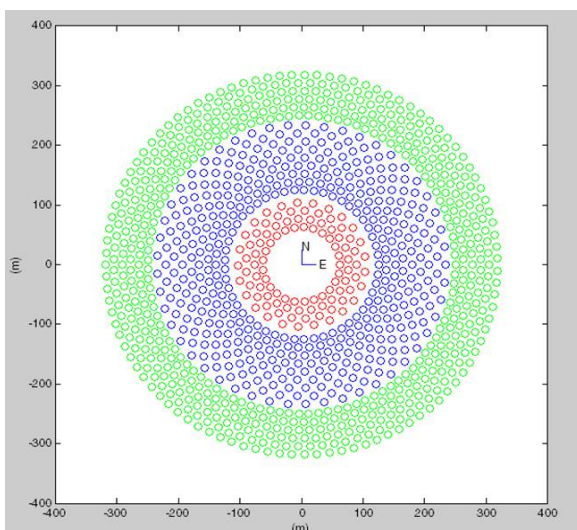


Figure 4. Field Layout for Radial Stagger Pattern

By creating a plot for Q_{tr} , the maximum value of thermal power received on the tower receiver is 78.973 MW_{th} during the month of July and the minimum value is 69.338 MW_{th} during the month of November, as shown in Figure 5.

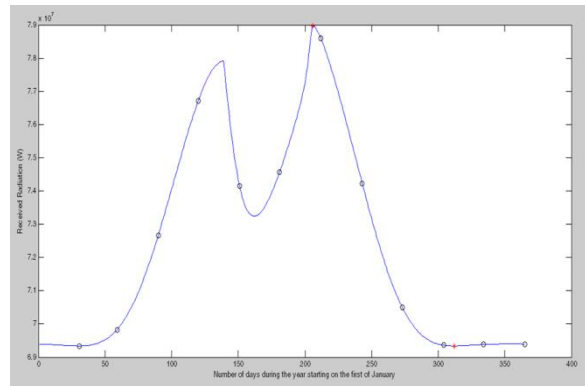


Figure 5. Solar thermal power on the tower receiver in each day of the year

CONCLUSIONS

In order to calculate the annual optical efficiency of a solar tower plant, a radial stagger pattern for the heliostat field layout was proposed in this paper. By using this pattern, the heliostat can be placed with a higher optical efficiency as well as a faster speed due to the fact that each heliostat could move freely and the heliostats standing between two heliostats of the first ring reduce the shadowing and blocking. According to the result of layout design, the annual optical efficiency of the heliostat field increases 2.36% when compared with the PS10 layout. In the process of solar thermal power design, the minimum value is greater than required thermal power. Thus, the excess thermal power can be stored for the electrical power production per day without solar radiation.

ACKNOWLEDGMENTS

The author would acknowledge to Dr. Yan Aung Oo, Professor and Head, Department of Electrical Power Engineering, Mandalay Technological University for her kindly permission and suggestion throughout the preparation of paper. Especially, the author would like to express deeply gratitude to her supervisor, Dr. Nang Saw Yuzana Kyaing, Lecturer, Department of Electrical Power Engineering, Mandalay Technological University for his valuable advice, encouragement help throughout the period of study. The author is deeply grateful to her parents who specially offered strong moral and physical support, care and kindness.

REFERENCES

- [1] K.-K. Chong and M.H. Tan, " Comparison Study of Two Different Sun-Tracking Methods in Optical Efficiency

- of Heliostat Field”, International Journal of Photoenergy, 2012.
- [2] Yiyi Zhou and Yuhong Zhao, “Heliostat Field Layout Design for Solar Tower Power Plant Based on GPU”, The Internal Federation of Automatic Control, pp.4953-4958, 2014.
- [3] Saeb M. Besarati and D. Yogi Goswami, “A Computationally Efficient Method for the Design of the Heliostat Field for Solar Power Tower Plant”, Renewable Energy, pp. 226-232, 2014.
- [4] Lipps, F.W., Vant-Hull and L.L., “A cell wise method for the optimization of large central receiver systems”, Solar Energy, pp. 505-16, 1978.
- [5] Francisco J. Collado, Jesús Guallar, “Campo: Generation of regular heliostat field”, pp. 49-59, 2012.
- [6] Mohammad Saghaififar, “Thermo- Economic Optimization of Hybrid Combined Power Cycles using Heliostat Field Collector”, Master Thesis of American University of Sharjah College of Engineering, 2016.
- [7] Maimoon Atif and Fahad A. Al-Sulaiman, “Development of a mathematical model for optimization a heliostat field layout using differential evolution method”, International Journal of Energy Research, 2015.
- [8] Chao Shen, et al., “Modelling and simulation of solar radiation data processing with Simulink”, Simulation Modelling Practice and Theory, pp. 721–735, 2008.
- [9] Kian Jazayeri, Sener Uysal and Moein Jazayeri, “MATLAB/Simulink Based Simulation of Solar Incidence Angle and the Sun’s Position in the Sky with Respect to Observation Points on the Earth”, Electrical and Electronic Engineering Department, Eastern Mediterranean University Famagusta, North Cyprus.
- [10] Yingxue Yao, Yeguang Hub and Shengdong Gao, “Heliostat field layout methodology in central receiver systems based on efficiency-related distribution”, Solar Energy, pp. 114-124, 2015.
- [11] Bason F., 2012, SolData Instrument, Available at soldata@soldata.dk.
- [12] John A. Duffie and William A. Beckman, “Solar Engineering of Thermal Processes”, Fourth Edition, Solar Energy Laboratory, University of Wisconsin-Madison, 2013.
- [13] Xiudong Wei, et al, “A new method for the design of the heliostat field layout for solar tower power plant”, Renewable Energy, pp. 1970–1975, 2010.

★ ★ ★